Biophysical Journal Volume 71 November 1996 2544–2552

Fast Voltage Clamp Discloses a New Component of Presteady-State Currents from the Na^+–Glucose Cotransporter

Xing-Zhen Chen,* Michael J. Coady,# and Jean-Yves Lapointe*

*Département de Physique and #Département de Physiologie, Groupe de recherche en transport membranaire, Université de Montréal, Montréal, Québec H3C 3J7, Canada

ABSTRACT The human Na^+–glucose cotransporter (hSGLT1) has been shown to generate, in the absence of sugar, presteady-state currents in response to a change in potential, which could be fitted with single exponentials once the voltage had reached a new constant value. By the cut-open oocyte technique (voltage rising-speed ~1 mV/μs), phlorizin-sensitive transient currents could be detected with a higher time resolution during continuous intracellular perfusion. In the absence of sugar and internal Na^+, and with 90 mM external Na^+ concentration ($[Na^+]_o$), phlorizin-sensitive currents exhibited two relaxation time-constants: τ_1 increased from 2 to 10 ms when V_m decreased from +60 mV to −80 mV and remained at 10 ms for more negative V_m; τ_2 ranged from 0.4 to 0.8 ms in a weakly voltage-dependent manner. According to a previously proposed model, these two time constants could be accounted for by 1) Na^+ crossing a fraction of the membrane electrical field to reach its binding site on the carrier and 2) conformational change of the free carrier. To test this hypothesis, the time constants were measured as $[Na^+]_o$ was progressively reduced to 0 mM. At 30 and 10 mM external Na^+, τ_1 reached the same plateau value of 10 ms but at more negative potentials (−120 and −160 mV, respectively). Contrary to the prediction of the model, two time constants continued to be detected in the bilateral absence of Na^+ (at pH 8.0). Under these conditions, τ_1 continuously increased through the whole voltage range and did not reach the 10 ms level even when V_m had attained −200 mV while τ_2 remained in the range of 0.4–0.8 ms. These results indicate that 1) conformational change of the free carrier across the membrane must occur in more than one step and 2) Na^+ binding/debinding is not responsible for either of the two observed exponential components of transient currents. By use of the simplest kinetic model accounting for the portion of the hSGLT1 transport cycle involving extracellular Na^+ binding/debinding and the dual-step conformational change of the free carrier, τ_1 and τ_2 were fitted throughout the voltage range, and a few sets of parameters were found to reproduce the data satisfactorily. This study shows that 1) τ_1 and τ_2 correspond to two steps in the conformational change of the free carrier, 2) Na^+ binding/debinding modulates the slow time constant (τ_1), and 3) a voltage-independent slow conformational change of the free carrier accounts for the observed plateau value of 10 ms.

INTRODUCTION

Na^+–glucose cotransport is found predominantly in the apical membrane of small intestine and kidney proximal tubules. It was specifically hypothesized in 1961 (Crane et al.), and since 1974 it has been studied extensively in epithelial cells and in brush border membrane vesicles (Murer and Hopfer, 1974; Semenza et al., 1984). In 1987, a cDNA clone (SGLT1) coding for a Na^+–glucose cotransporter was isolated from a rabbit small-intestinal library and expressed successfully in *Xenopus laevis* oocytes (Hediger et al., 1987). This preparation has allowed an electrophysiological characterization, leading to a detailed kinetic model (Parent et al., 1992b). SGLT1 clones were later obtained from human, rat, sheep, and pig (Hediger et al., 1989; Lee et al., 1994; Tarpey et al., 1994; Ohta et al., 1990). cDNA clones expressing related cotransporters with a lower affinity for glucose have also been isolated (Mackenzie et al., 1994; Hediger and Rhoads, 1994).

SGLT1 couples the transport of two sodium ions to one glucose molecule (Chen et al., 1995), and several models have been proposed to explain how Na^+ energizes the transport of glucose (Schultz and Curran, 1970; Crane, 1977; Restrepo and Kimmich, 1985; Kimmich and Randles, 1988; Parent et al., 1992b; Loo et al., 1993). Even with the simplifying assumption that the three substrates bind to the transporter in an ordered manner from each side of the membrane, the kinetic model remains complicated and must deal with forward and backward rate constants among the eight different states of the carrier (i.e., free, partially loaded, or fully loaded carrier). Fortunately, SGLT1 can be studied in the absence of glucose, where it demonstrates transient currents. In fact, when a voltage pulse is applied across the membrane, mobile charged residues and charged substrates of a membrane transporter are able to move within the membrane electrical field and attain new equilibrium positions, generating a transient current (also called a presteady-state current, or a gating current for voltage-sensitive channels) (Parent et al., 1992a,b). In this simplified kinetic model, if n distinct conformational states are involved in the process, the presteady-state current can be expressed as a sum of $n - 1$ exponential components. Na^+–K^+ ATPase (Nakao and Gadsby, 1986; Rakowski, 1993; Hilgemann, 1994), the Na^+–Ca^{2+} exchanger (Hilgemann et al., 1991), and a cationic amino acid transporter

Received for publication 12 July 1996 and in final form 13 August 1996.

Address reprint requests to Dr. Jean-Yves Lapointe, GRTM, Département de Physique, Université de Montréal, C.P. 6128, Succursale "Centre-Ville," Montréal, Québec H3C 3J7, Canada. Tel: 514-343-7046; Fax: 514-343-7146; E-mail: lapoinj@ere.umontreal.ca.

0006-3495/96/11/2544/09 $2.00

(Klamo and Kavanaugh, 1995) have also been shown to generate presteady-state currents. In the case of rabbit and human SGLT1, one time constant has been identified in a limited voltage range (from +50 to −50 mV) by use of a two-microelectrode voltage-clamp technique that has a typical time resolution of 2 ms (Parent et al., 1992a; Loo et al., 1993). In a preliminary report (Loo et al., 1994), a faster component producing an initial rising phase has also been identified.

In the present study, transient phlorizin- (Pz-) sensitive currents were measured by the cut-open oocyte technique, which demonstrates a time resolution of better than 200 μs and allows accurate control of the solutions bathing both surfaces of the oocyte membrane (Taglialatela et al., 1992; Costa et al., 1994; Chen et al., 1995). After the application of extracellular glucose to verify SGLT1 expression, stepwise alteration of conditions on both sides of the membrane permitted association of the transient currents with conformational changes of the transporter. First, intracellular Na^+ and glucose were removed (absolute zero *trans* conditions); second, extracellular glucose was removed and extracellular Na^+ was progressively replaced by *N*-methyl-D-glucamine. In the bilateral absence of glucose and Na^+, all existing kinetic models for Na^+–glucose cotransport (Schultz and Curran, 1970; Crane, 1977; Restrepo and Kimmich, 1985; Kimmich and Randles, 1988; Parent et al., 1992b; Loo et al., 1993) can be simplified to a two-state model. Thus measurements of the sole time constant at various membrane potentials should directly determine the two rate constants of the free-carrier conformational change. Current models (Parent et al., 1992b; Kimmich and Randles, 1988) predict that the addition of extracellular Na^+ should cause a three-state model, and two time constants should be observed. Although we did measure two time constants in the presence of external Na^+ across an extended voltage range (from +60 to −200 mV), we were surprised to find that transient currents continued to display both time constants when external Na^+ was reduced to zero. This observation necessitates a minimal three-state model for conformational changes of the free transporter. This model is shown to reproduce satisfactorily our experimentally derived results.

MATERIALS AND METHODS

Oocyte preparation

Oocytes were prepared as previously described (Chen et al., 1995). The follicular layer was removed by collagenase treatment in a Ca^{2+}-free solution, and defolliculated oocytes were incubated in Barth's solution, consisting of 90 mM NaCl, 3 mM KCl, 0.82 mM $MgSO_4$, 0.41 mM $CaCl_2$, 0.33 mM $Ca(NO3)_2$, and 5 mM HEPES, pH 7.60. 300 pg of pMT21-SGLT1, a recombinant eukaryotic expression vector bearing a full-length human SGLT1 cDNA (Chen et al., 1995), together with 300 pg of pMT21-GFP as a fluorescent marker for cDNA expression (Coady et al., 1996), were used for nuclear injection in *Xenopus laevis* oocytes 1 day after defolliculated oocytes were obtained. After 3–7 days of incubation at 18°C in a modified Barth solution (Quick et al., 1992), fluorescent oocytes were selected (Coady et al., 1996) for cut-open oocyte experiments. In some experiments, oocytes injected with 5–15 ng of capped and polyadenylated hSGLT1 mRNA were also used, but no differences in the transient current characteristics from cDNA-injected oocytes were noted.

Cut-open oocyte technique

The technique used was similar to one previously described (Chen et al., 1995). Modifications made to the previous configuration include 1) the use of a microelectrode filled with 3 M KCl (resistance 0.5–2 MΩ) to clamp the membrane potential more accurately during the first few milliseconds of voltage pulses and 2) reduction of the feedback resistor in the amplifier head stage (100 kΩ instead of 10 MΩ) to increase the voltage rising-speed. With this modified system the voltage rising-speed was close to 1 mV/μs, with an additional 50 μs needed to stabilize membrane potential completely, following a small overshoot (see Fig. 1). For the largest pulse of 270 mV (from +70 to −200 mV), the time needed for potential stabilization was ~350 μs. The extracellular solutions contained 90 mM (cyclamic acid Na salt + cyclamic acid free base), 6.2 mM HCl, 1 mM $MgCl_2$, 0.9 mM $CaCl_2$, 10 mM HEPES, 30 mM Mannitol, and 0–90 mM *N*-methyl-D-glucamine, to yield a pH of 8.0. The intracellular solutions differed from the extracellular solutions in that they contained 1 mM EGTA and no Na^+.

Data acquisition and analysis

Data acquisition, storage, and analysis were performed with commercially available software (Pclamp 6.02, Axon Instruments, Inc., Foster City, CA).

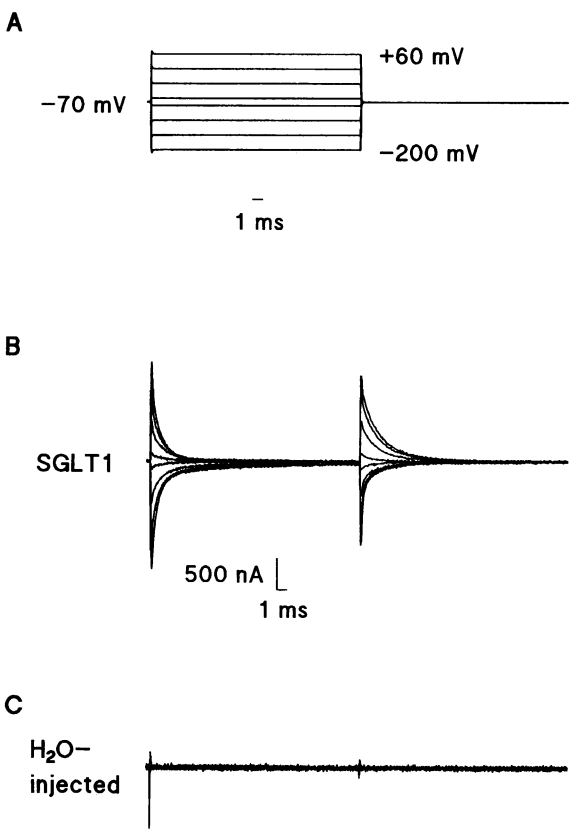

FIGURE 1 Example of applied voltage pulses and Pz-sensitive currents obtained by the cut-open oocyte technique. (*A*) V_m rises at a speed of ~1 mV/μs, and the new potential levels are reached within 150 μs from a conditioning potential of −70 mV. (*B*) The currents shown represent the differences between total currents measured before and 5–15 s after addition of Pz in an oocyte expressing SGLT1. (*C*) Pz-sensitive currents form in a H_2O-injected oocyte. In this example, $[Na^+]_o$ = 10 mM, [Pz] = 2 mM.

The sampling rate was set to 12 μs/point when only currents were measured and to 24 μs/point when both the membrane potentials and currents were measured. Transient currents were fitted by the Chebyshev method with either one or two exponential functions. For a given series of voltage pulses, transient currents were fitted from a time when all voltage pulses had completely stabilized, i.e., at t = 200–400 μs, and for a duration of 20–40 ms. We measured transient currents at membrane potentials ranging from +60 to −200 mV, using different preconditioning potentials (40 ms duration) to ensure that all voltage steps used in the analysis were larger than 90 mV to obtain a large amplitude for every transient current.

Adjustment of parameters from the kinetic model to fit experimental data was performed with a computer program written for this task in QuickBASIC (version 4.0, Microsoft, Redmont, WA). The program used a least-squares method to fit τ_1 with individual weighting (proportional to the inverse of the standard error of the mean of experimental values), whereas the weakly voltage-dependent τ_2 was simply required to be 0.4–0.8 ms throughout the voltage range. There were 12 parameters to be adjusted, each having a predefined interval and employing 5–12 different values, totaling 10^9 different combinations. For each combination, if the predicted τ_2 was satisfactory, then the root-mean-square deviation (σ) of τ_1 was calculated. Fifty to one hundred hours were needed to tour all possibilities when this program was run on a 486 100-MHz personal computer. After one search tour, unfavorable parameter regions (those returning large σ values) were eliminated, permitting the running of a new search cycle based on narrowed parameter intervals, thus yielding a more precise fit. Satisfactory fits were chosen after different favorable regions had been explored for three to five iterations.

RESULTS

In the absence of both glucose and intracellular Na^+, SGLT1 displays a transient Pz-sensitive current that can be easily detected by the cut-open oocyte technique (Fig. 1). It will be shown below that the transient current following a voltage pulse is due to reorientation of the free carrier and the binding/debinding of external Na^+, which has to cross a fraction of the membrane electrical field to reach its binding site. No significant Pz-sensitive transient current could be detected in water-injected oocytes (Fig. 1 *C*).

According to a current model (Loo et al., 1993), the SGLT1 transient currents in the presence of 90 mM external Na^+ are the sum of two exponential components ($I(t) = A_1\exp(-t/\tau_1) + A_2\exp(-t/\tau_2)$, where A_1 and A_2 are the amplitudes with time constants τ_1 and τ_2, respectively). Fig. 2A shows that, for arbitrarily selected voltage pulses, adequately fitting modeled curves to the transient currents recorded by the cut-open oocyte technique absolutely requires two exponential components. The potential dependence of the two time constants is shown in Fig. 2 *B* for a typical experiment. It was consistently observed that τ_1 (slower relaxation constant) increases as V_m becomes more negative and reaches a maximal value of 10 ms at $V_m \approx -80$ mV. At positive potentials the two time constants approach each other, and a monoexponential fitting may be suitable in this region of membrane potentials.

In the next series of experiments we sought to measure transient Pz-sensitive currents as $[Na^+]_o$ was progressively reduced to 0 mM. However, Pz can bind to SGLT1 only in the presence of sodium (Semenza et al., 1984) or protons (Hirayama et al., 1994). To avoid unwanted interference by H^+ (K_m for protons is 3 μM, or 5.5 pH units, for rabbit

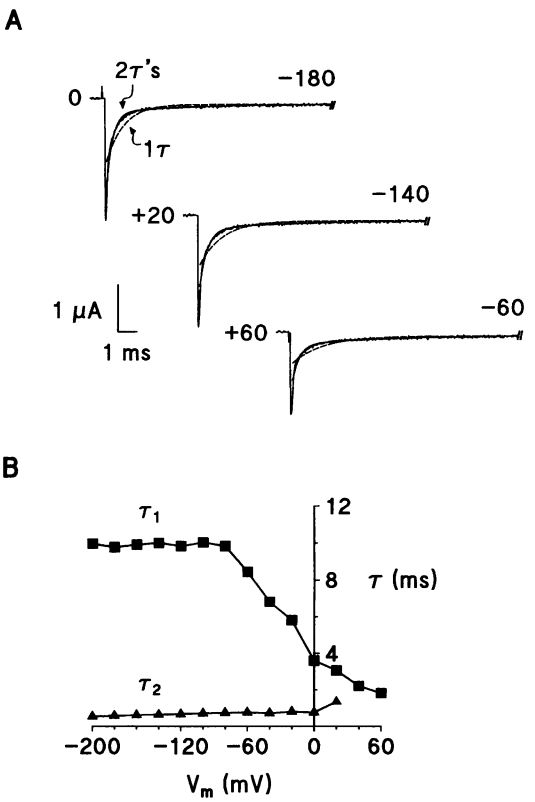

FIGURE 2 SGLT1 transient currents and associated time constants with $[Na^+]_o$ = 90 mM. (*A*) Representative current recordings, with solid curves representing two-exponential fit and dashed curves representing a monoexponential fit. (*B*) Voltage dependence of time constants derived from two-exponential fits at varied membrane potentials.

SGLT1 (Hirayama et al., 1994) and 0.4 μM, or 6.3 pH units, for human SGLT1 (unpublished data from our laboratory)), our solutions were adjusted to pH 8.0 in all experiments. To obtain SGLT1 transient currents in the bilateral absence of Na^+, we used the difference between total currents measured with 0 mM external Na^+ and currents recorded with the cotransporters blocked by use of 10 mM external Na^+ + 2 mM Pz. To justify the adequacy of this procedure, we first verified that the external addition of 10 mM Na^+ did not generate transient currents in control oocytes. In five experiments with H_2O-injected oocytes from four donors, transient currents generated by the external addition of 10 mM Na^+ (Fig. 3 *D*) were negligible compared with SGLT1-specific transient currents obtained with 90 mM Na^+ (Fig. 3 *A*), 30 mM Na^+ (Fig. 3 *B*), and 0 mM Na^+ (Fig. 3 *C*). The negligible amplitude of the transient currents induced by external addition of 10 mM Na^+ to water-injected oocytes can be more clearly appreciated by comparison of the charge transferred (Fig. 3 *E*). Also, the Pz inhibition constant (K_i) for human SGLT1 was shown to be 0.2 μM (Jalal et al., 1996) in the presence of 90 mM Na^+, and measurement of the Pz-sensitive sodium leak (unpublished data) indicated that, at 5 mM Na^+, 0.1 mM Pz had completely blocked the sodium leak. Thus, Pz-sensitive currents in the

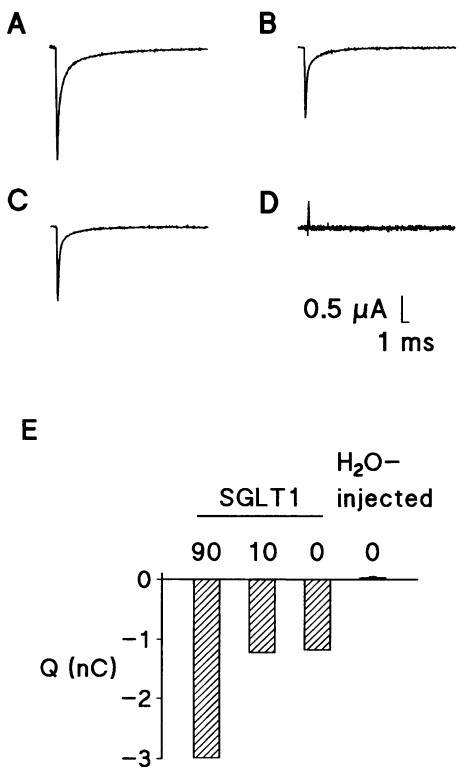

FIGURE 3 External Pz-sensitive transient currents and charge transfers. The voltage pulse ranged from +60 to −60 mV.(*A–C*) Pz-sensitive transient currents from the same SGLT1-injected oocyte. (*D*) Transient current from a water-injected oocyte. Transient currents were recorded with (*A*) 90 mM Na^+ ± 0.5 mM Pz, (*B*) 10 mM Na^+ ± 2 mM Pz, and (*C*, *D*) 0 mM Na^+ ± (10 mM Na^+ + 2 mM Pz). (*E*) Charge transfers calculated from the above individual transient currents, except that the charge transfer in H_2O-injected oocytes represents an average from five oocytes originating from four different donors.

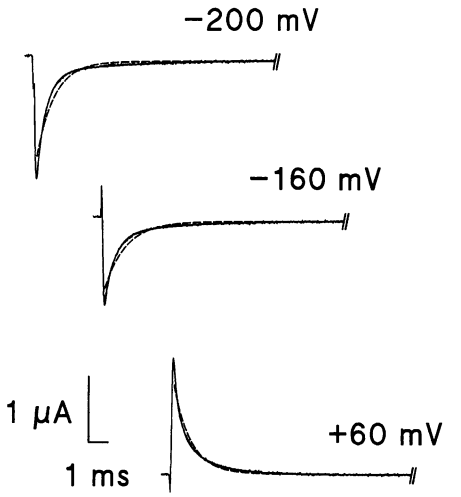

FIGURE 4 Examples of SGLT1 transient currents in the absence of Na^+. Voltage pulses range from −70 mV to different values. Solid curves represent two-exponential fit; dashed curves represent the best monoexponential fit.

absence of Na^+ can be accurately measured by inhibition with 10 mM Na^+ + 2 mM Pz.

Unexpectedly, SGLT1 transient currents continued to be a sum of two exponential components in the absence of Na^+ (Fig. 4) rather than monoexponential as predicted by existing models (Schultz and Curran, 1970; Crane, 1977; Restrepo and Kimmich, 1985; Kimmich and Randles, 1988; Parent et al., 1992b; Loo et al., 1993). As shown in Fig. 4, monoexponential fitting is as clearly unsatisfactory as it had been for 90 mM external Na^+. For 5–9 oocytes the determination of time constants was performed at extracellular Na^+ concentrations of 90, 30, 10, and 0 mM. The slow constant (τ_1) attained the same plateau value of 10 ms at increasingly negative potentials as $[Na^+]_o$ was reduced (Fig. 5). In the absence of Na^+ this saturation is not attained, even at −200 mV (Fig. 5 *D*). τ_2 ranged between 0.4 and 0.8 ms, was less dependent on the membrane potential than τ_1, and was little affected by the extracellular Na^+ concentration.

The presence of two time constants in the absence of Na^+ suggests that charge translocating conformational changes of the free carrier must occur in at least two distinct steps. None of the previously proposed models can account for such an observation, and a new model describing the four states of the transporter in the absence of glucose and intracellular Na^+ is proposed in Fig. 6 *A* (Refer to Eq. A1 in Appendix A for the detailed expressions for pseudo-rate constants k_{ij}). To keep the model as simple as possible, we assumed a single sodium ion binding to the external site. Although two sodium ions are cotransported with one glucose molecule (Chen et al., 1995), so far there is no evidence that two sodium ions participate in the transient currents found in the absence of glucose. The model parameters were adjusted to fit the experimental time constant data (see Materials and Methods). In total, 30 sets of parameters giving an acceptable fit (0.35 ms $\leq \sigma \leq$ 0.37 ms) were kept. Among these sets of parameters, the values for k_{12}^0, k_{21}^0, k_{23}^0, and k_{32}^0 varied in a narrow range of ±10%, the symmetry parameters of energy barriers α_i and apparent valences z_i (i = 1, 2, 3) varied within ± 20%, and, although k_{34}^0 and k_{43}^0 describing external Na^+ binding and debinding varied by 3–5-fold, the ratio k_{43}^0/k_{34}^0 remained within a ± 50% variation. After we compared the predicted amplitudes of both exponential components with their experimental values, 25 sets could be eliminated. The best set was selected among the remaining five based on a visual inspection of the quality of the fit for τ_2. The set of parameter values with the best fit (Fig. 6 *B*) gives a satisfactory fit to both time constants, and this fit is shown in Fig. 5 by the solid curves. This set of parameters also satisfactorily predicts the amplitudes of the two components of transient currents versus V_m (Fig. 7 *A*) as well as charge transfers versus V_m (Fig. 7 *B*). An interesting feature of the best parameter set (as was the case for all 30 acceptable sets) is that the second outward translocation (k_{23}) is independent of membrane potential (because $\alpha_2 = 0$; see Eq. A1 in Appendix A) and is responsible for the limiting value (10 ms)

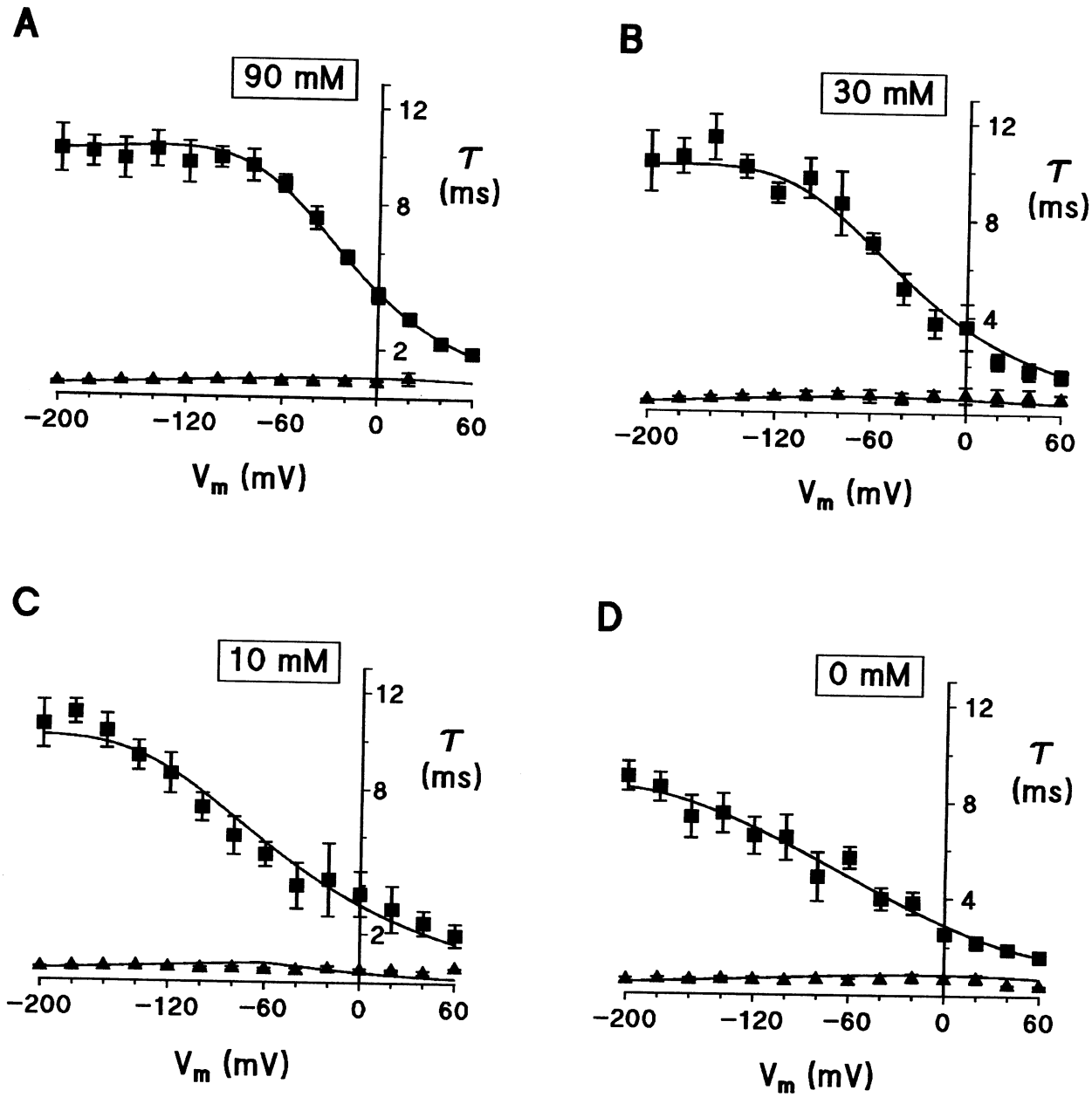

FIGURE 5 Voltage dependence of the two time constants needed to fit the transient currents at different $[Na^+]_o$. Average values (±SE) from five to nine oocytes are shown as data points; solid curves represent the best fit of the model shown in Fig. 6 *B*. ■, τ_1; ▲, τ_2.

reached by τ_1 at very negative V_m. The other two energy barriers are rather symmetrical as $\alpha_1 = 0.3$ and $\alpha_3 = 0.4$. The total valence associated with the conformational changes of the free carrier is z_1 (-0.4) + z_2 (-0.35) = -0.75, which represents only half of the valence previously proposed (-2×0.7 in Parent at al. (1992b) and in Loo et al. (1993)), whereas the valence value of z_3 ($=-0.6$) associated with the external Na^+ binding/debinding is consistent with those in previous reports. The voltage dependence of these steps is in agreement with the results of earlier studies of the intestinal Na^+–glucose cotransporter (Semenza et al., 1984; Bennett and Kimmich, 1992, 1996). As we can see from Eq. A2 (Appendix A), τ_1 corresponds to the second step of the free-carrier translocation ($E_2 \Leftrightarrow E_3$), but the fast and strongly voltage-dependent binding/debinding (k_{34}/k_{43}) modifies the τ_1-versus-V_m profile as a function of $[Na^+]_o$. With the current parameter set, $\tau_2 \approx 1/(k_{12} + k_{21})$ (Eq. A2) and corresponds to the first step of the free-carrier translocation ($E_1 \Leftrightarrow E_2$); τ_2 is not influenced by the distant external Na^+ binding/debinding reaction.

DISCUSSION

Using the cut-open oocyte technique, we observed two time constants in the presence of external Na^+ for a large mem-

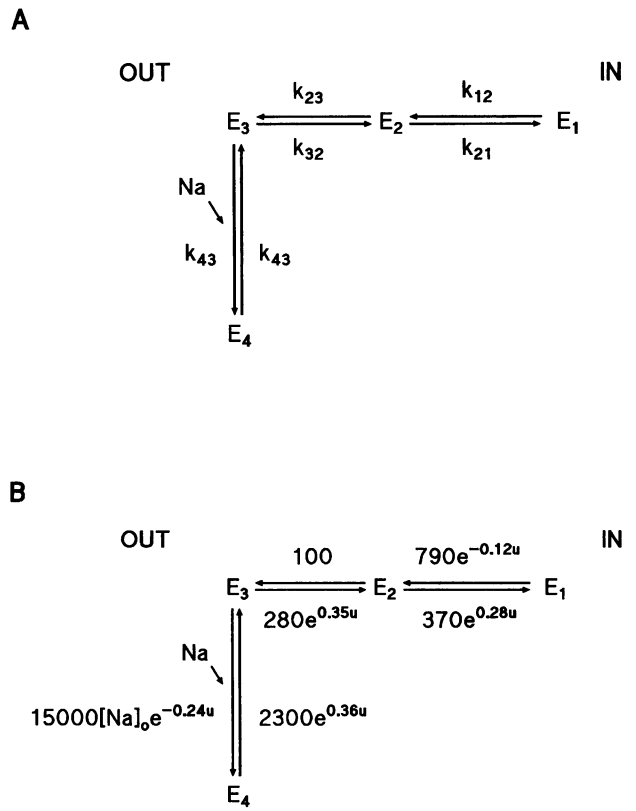

FIGURE 6 Four-state kinetic model for SGLT1 in the absence of substrates. (*A*) Translocation of a free carrier across the membrane is described by the transitions between states E_1 (facing in), E_2 (intermediate state), and E_3 (facing out). The binding and debinding of external Na^+ to the carrier are described by transition between E_3 and E_4. (*B*) Parameter values are from the set that gave the fit shown in Fig. 5. u represents reduced membrane potential (Eq. A1). The energy barrier between E_2 and E_3 is totally asymmetrical ($\alpha_2 = 0$).

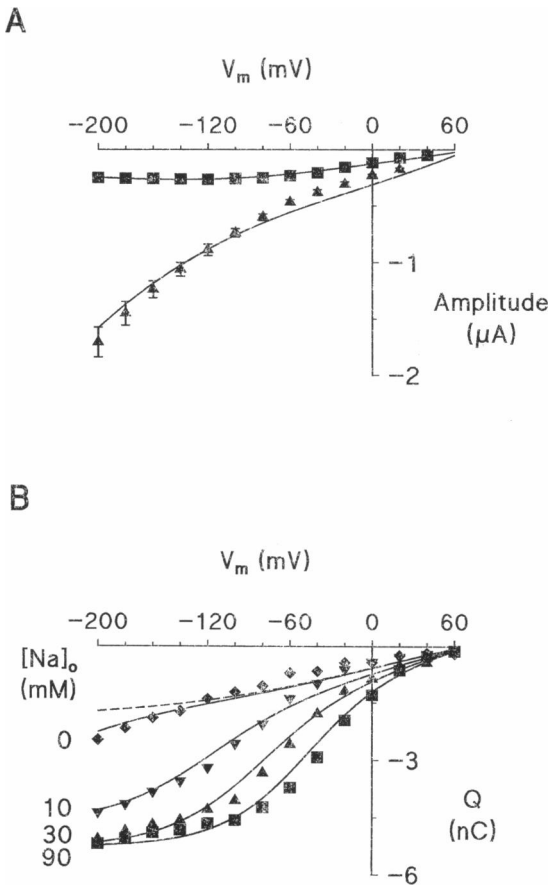

FIGURE 7 Model's prediction of amplitudes of exponential currents and charge transfers as functions of membrane potential. The voltage pulses were from +70 mV to different values ranging from +60 to −200 mV. Predicted and experimental results are indicated, respectively, by curves and data points. (*A*) Amplitudes corresponding to the slow time constant (■, τ_1) and to the fast time constant (▲, τ_2) were obtained with $[Na^+]_o$ = 90 mM. (*B*) Charge transfers were measured with various extracellular Na^+ concentrations as indicated in the figure; in the case of 0 mM external Na^+, dashed and solid curves represent the model's predictions with 0 and 0.5 mM external Na^+, respectively.

brane potential range (Fig. 5 *A–C*, from +60 to −200 mV), consistent with the predictions of a recent model (Loo et al, 1993). The slow time constant measured here (τ_1; Fig. 5) was in accordance with the experimental data previously published, which were obtained across a limited voltage range (+50 to −50 mV). However, at more negative potentials the observed slow time constant value remained at the 10 ms level, whereas the previous model predicted a progressive decrease toward low values. More importantly, the presence of two time constants in the transient currents recorded in the bilateral absence of Na^+ and glucose was clearly demonstrated in our experiments, indicating that the conformational changes of the free carrier across the membrane involve the movement of charged residues in the membrane electrical field in at least two distinct steps.

The 30 sets of parameters that best fit our model concur that the plateau value of 10 ms for τ_1 at very negative potentials is determined by the voltage-independent rate constant k_{23} of 100 s^{-1}. Therefore, τ_1 is associated with free-carrier translocation between the intramembrane state E_2 and the outward-facing state E_3. τ_2 is associated with the translocation between E_1 and E_2. The behaviors of τ_1 and τ_2 as functions of V_m and $[Na^+]_o$ are best understood when approximate expressions are used (Eq. A2). Theoretically, the time constant associated with a rapid step is determined solely by the two rate constants of that step (it is equal to the inverse of the sum of the two rate constants), but the time constant associated with a slow step is also modified by rate constants from neighboring rapid steps (see the expression for τ_1 in Eq. A2). Therefore, the presence of the two voltage-dependent modulation factors f_{12} ($=k_{12}/(k_{12} + k_{21})$) and f_{43} ($=k_{43}/(k_{34} + k_{43})$) in the expression for τ_1 increases the voltage dependence of τ_1. Moreover, with the parameters in Fig. 6 *B*, $\tau_1 \rightarrow 1/k_{23} = 10$ ms when $V_m \rightarrow -\infty$; $\tau_1 \rightarrow 0$ when $V_m \rightarrow +\infty$. In the absence of external Na^+, the model predicts that τ_1 will reach 10 ms only at $V_m \leq -350$ mV. When $[Na^+]_o$ is high, the term $f_{43} \cdot k_{32}$ approaches zero at less negative potentials and, consequently, τ_1 also reaches 10 ms at less negative potentials. In contrast, to a first-

degree approximation, τ_2 is independent of external Na^+ binding/debinding, which explains why, experimentally, it is little affected by $[Na^+]_o$ and is less voltage dependent than τ_1.

We have seen that a four-state model can adequately describe our experimental data on time constants and exponential current amplitudes as well as predict charge transfers. There are actually three different τ in the presence of external Na^+, where the third (τ_3) is associated with binding and dissociation of external Na^+. However, when $[Na^+]_o$ = 90 mM, τ_3 lies between 0.1 and 0.3 ms, at the limit of our time resolution; with 30 mM external Na^+, τ_3 is in the range of τ_2, and with 10 mM external Na^+, τ_3 is between τ_1 and τ_2. In the latter two conditions, fitting experimental data with a sum of three exponential components has been unreliable because the three different τ are too close to one another, particularly at positive potentials, where fitting with two exponential components is difficult.

Despite the fact that two sodium ions are cotransported with one glucose molecule, it is uncertain whether both of the sodium ions are involved in the generation of transient currents recorded in the absence of glucose. In addition to the "best fit" parameters shown in Fig. 6 *B*, for which a model with one Na^+ binding to the transporter has been assumed, we have also found a set of parameters, based on the simultaneous binding of two sodium ions (data not shown), that satisfactorily fits the experimental data shown in Fig. 5 and accurately predicts amplitudes versus V_m. Hence, the information contained in time constants is not sufficient to permit us to distinguish between models with one Na^+ binding, as proposed by Kimmich and Randles (1988), and two simultaneous Na^+-binding models (Parent et al., 1992b) in the absence of glucose.

As SGLT1 is capable of using external protons in place of external Na^+ to cotransport glucose (Hirayama et al., 1994), we have to consider the possibility that the external H^+ binding/debinding may influence our measurements, especially in the absence of external Na^+. For human SGLT1 the affinity for external protons is close to 0.4 μM (pH 6.3) in the absence of glucose. At pH 8.0, the proton concentration is ~2% of its K_m, and this is why, in Fig. 7 *B*, predicted values with 0.5 mM external Na^+ are also shown (~2% of its K_m). Although the prediction with 0.5 mM external Na^+ better fits the data obtained with nominally Na^+-free conditions, the conclusion that the observed two relaxation time-constants are associated with free-carrier translocation but not with external Na^+ binding/debinding remains unchanged. Theoretically, the time constant value associated with external Na^+ binding/debinding at very negative membrane potentials should increase severalfold when $[Na^+]_o$ decreases from 90 to 10 mM; this is not the case for the two observed time constants (Fig. 5). Numerically, simulation has been performed on the three-state model of Loo et al. (1993), for which either one external Na^+ binding or two simultaneous Na^+ bindings had been considered, but not a single parameter set could be found to fit our experimental data satisfactorily with 10, 30, and 90 mM external Na^+.

The z_i values obtained from fitting can be used to calculate the number (N_t) of SGLT1 transporters in the membrane (see Appendix B). The example shown in Fig. 7 *B* with $[Na^+]_o$ = 90 mM gives a Q_{max} of 5.6/0.08 nC. The factor of 0.08 is a consequence of the membrane patch isolated for measurement, representing ~8% of the total membrane surface if a uniform distribution of carriers in the membrane is assumed. According to Eq. B2, we have

$$N_t = Q_{max}/e|Z| = 5.6 \times 10^{-9}/(0.08 \times 1.35 \times 1.6 \times 10^{-19}) = 3.5 \times 10^{11} \text{ carriers/oocyte},$$

where $Z = z_1 + z_2 + z_3 = -1.35$. It should be noted that, if the number of states in a model is more than two, more than one valence parameter z has to be used, and the Boltzmann formula is no longer appropriate to describe charge transfer versus membrane potential because it assumes a single valence z. As an example, when the Boltzmann formula is used to fit Q versus V_m for $[Na^+]_o$ = 90 mM, a single z value of -0.8 or -0.7, respectively, is obtained from experimental data or from our model's prediction (Fig. 7 *B*). In fact, the single z here represents, to some extent, an average effect of three z_i and therefore is much smaller than the sum of the three (-1.35). In addition, this single z tends to diminish as the $[Na^+]_o$ decreases, which is inexplicable either by our model or by that proposed by Loo et al. (1993). As two external sodium ions cross the entire membrane potential after a complete cotransport cycle, the sum of all valences associated with each voltage-dependent step along this cycle must be -2. Therefore, some other steps (binding/debinding of the second external Na^+ or of intracellular Na^+ or translocation across the membrane of the fully loaded carrier) must be voltage dependent, with a total valence of -0.65.

To assess the relative importance of the four states (E_1, E_2, E_3, and E_4), we calculated occupation probabilities after a pulse from -50 to $+50$ mV under conditions of 90 mM external Na^+ (Fig. 8 *A*) and 0 mM external Na^+ (Fig. 8 *B*), using the rate constants shown in Fig. 6 *B*. At -50 mV, carriers distribute near the extracellular face of the membrane, but only $E1$ is negligible; at $+50$ mV, carriers distribute equally in states E_1 and E_2 near the intracellular face, with negligible E_3 and E_4. This shows that neither of the E_1 and E_2 configurations, which were previously lumped together, can be neglected in this voltage range.

In summary, fast voltage-clamp experiments using the cut-open oocyte technique have identified two exponential components of SGLT1 transient currents, even in the bilateral absence of Na^+. This is a "direct" indication that free-carrier translocation across the membrane occurs in at least two distinct steps. In the proposed model, the slow relaxation constant (τ_1) corresponds to the free-carrier translocation between E_2 and E_3, whereas the fast constant (τ_2) corresponds to the transition between E_1 and E_2. The addition of 90 mM external Na^+ modifies τ_1 in such a way that it becomes more voltage dependent and that it reaches the

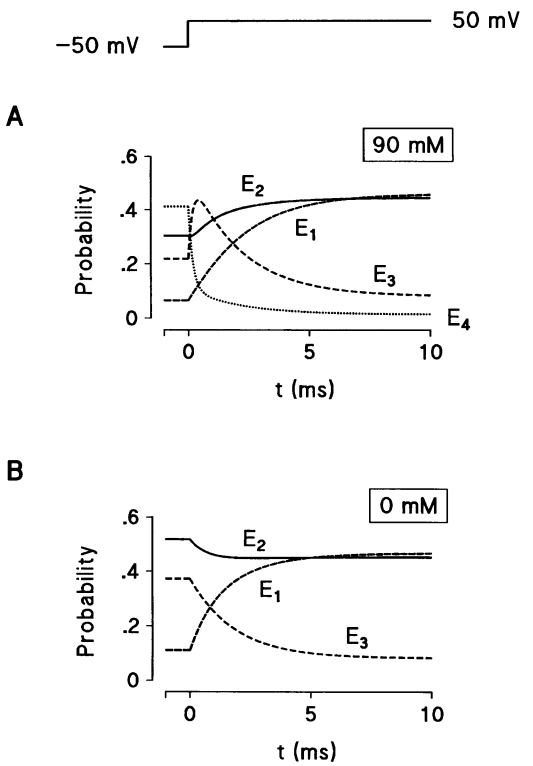

FIGURE 8 Time course of occupation probabilities following a voltage pulse. Occupation probabilities are calculated with the values shown in Fig. 6 *B* for $[Na+]_o$ of (*A*) 90 mM and (*B*) 0 mM. Probability profiles show that all three free-carrier states (E_1, E_2, and E_3) represent significant proportions of the SGLT1 population in the voltage range between −50 and +50 mV.

maximal value of 10 ms at a less negative membrane potential (≈80 mV), whereas τ_2 is little affected by external Na^+ binding/debinding, in accordance with the model's prediction.

APPENDIX A. EXPRESSIONS FOR k_{ij} AND RELAXATION TIME-CONSTANTS τ

Based on Eyring rate theory, the pseudo rate constants k_{ij} in Fig. 4 *A* can be written as follows:

$$k_{12} = k_{12}^0 \exp(z_1\alpha_1 u), \qquad k_{21} = k_{21}^0 \exp[-z_1(1-\alpha_1)u],$$
$$k_{23} = k_{23}^0 \exp(z_2\alpha_2 u), \qquad k_{32} = k_{32}^0 \exp[-z_2(1-\alpha_2)u],$$
$$k_{34} = [Na^+]_o k_{34}^0 \exp(z_3\alpha_3 u), \qquad k_{43} = k_{43}^0 \exp[-z_3(1-\alpha_3)u], \tag{A1}$$

where $u = FV_m/RT$; F, R, and T have their usual meanings; at a working temperature of T = 22°C, u = 0.0394 V_m (mV). z_i represents charge valence (equivalent charge crossing the whole membrane) of the step between E_i and E_{i+1}; α_i (between 0 and 1) describes the asymmetry of energy barriers, and k_{ij}^0 are rate constants. The units of k_{ij}^0 are in s^{-1}, except that k_{34}^0 is in $s^{-1}\,M^{-1}$.

Exact expressions for the three τ corresponding to the model shown in Fig. 6 *A* are complex, as they are roots of a general third-degree polynomial whose coefficients are functions of k_{ij}. However, approximate expressions for τ_1, τ_2, and τ_3 can be obtained under the conditions $k_{12} + k_{21} \gg k_{23} + k_{32} \ll k_{34} + k_{43}$, consistent with the best set of parameter values shown in Fig. 6 *B*:

$$\tau_1 \approx \frac{1}{f_{12}\cdot k_{23} + f_{43}\cdot k_{32}},$$
$$\tau_2 \approx \frac{1}{k_{12} + k_{21}}, \tag{A2}$$
$$\tau_3 \approx \frac{1}{k_{34} + k_{43}},$$

where f_{12} ($=k_{12}/(k_{12} + k_{21})$) and f_{43} ($=k_{43}/(k_{34} + k_{43})$) are modulating factors for τ_1 from the steps $E_1 \Leftrightarrow E_2$ and $E_3 \Leftrightarrow E_4$, respectively.

APPENDIX B. EXPRESSIONS FOR CHARGE TRANSFER Q AND FOR THE NUMBER OF CARRIERS N_t

Consider an n-state kinetic model across the membrane:

$$\text{OUT} \quad E_n \overset{z_{n-1}}{\Longleftrightarrow} E_{n-1} \overset{z_{n-2}}{\Longleftrightarrow} \cdots \cdots \overset{z_2}{\Longleftrightarrow} E_2 \overset{z_1}{\Longleftrightarrow} E_1 \quad \text{IN}.$$

Then the charge transfer can expressed as

$$Q(V_m) = N_t e \sum_{i=2}^{n} \left(\sum_{j=1}^{i-1} z_j \right)(E_i - E_{0i}) = N_t e \sum_{i=2}^{n} \left(\sum_{j=1}^{i-1} z_j \right) E_i + C, \tag{B1}$$

where E_{0i} and E_i are occupation probabilities at initial potential V_0 and new potential V_m, respectively, z_i are effective valences between E_i and E_{i+1}, $e = 1.6 \times 10^{-19}$ C (elementary charge constant), and C is a constant that depends only on initial conditions. Assume that the free carrier is negatively charged and that all z_i are nonzero (for the purpose of charge transfer calculus, any two states (E_i and E_{i+1}) with voltage-independent transitions between them, i.e., $z_i = 0$, can be replaced by a state E_i' such that $E_i' = E_i + E_{i+1}$). Thus, when $V_m \to -\infty$, $E_i \to 0$ for $i = 1 \ldots n-1$ and $E_n \to 1$; when $V_m \to +\infty$, $E_i \to 0$ for $i = 2 \ldots n$ and $E_1 \to 1$. As well,

$$Q(-\infty) = N_t e \left(\sum_{j=1}^{n-1} z_j \right) + C = N_t e Z + C.$$

$$Q(+\infty) = C$$

We obtain the following expression for the number of carriers:

$$N_t = Q_{max}/e|Z| \tag{B2}$$

where

$$Q_{max} = Q(+\infty) - Q(-\infty), \qquad Z = \sum_{j=1}^{n-1} z_j.$$

We thank Ms. Bernadette Wallendorff for excellent technical assistance. This research is supported by the Medical Research Council of Canada (grant MT-10580 awarded to J.Y.L.).

REFERENCES

Bennett, E., and G. A. Kimmich. 1992. Na^+ binding to the Na^+-glucose cotransporter is potential dependent. *Am. J. Physiol.* 262:C510–C516.

Bennett, E., and G. A. Kimmich. 1996. The molecular mechanism and potential dependence of the Na^+/glucose cotransporter. *Biophys. J.* 70:1676–1688.

Chen, X.-Z., M. J. Coady, F. Jackson, A. Berteloot, and J.-Y. Lapointe. 1995. Thermodynamic determination of the Na^+:glucose coupling ratio for the human SGLT1 cotransporter. *Biophys. J.* 69:2405–2414.

Coady, M. J., G. Lemay, and J.-Y. Lapointe. 1996. Use of green fluorescent protein cDNA as a marker for nuclear injection of *Xenopus laevis* oocytes. *FASEB J.* 10:A89.

Costa, A. C. S., J. W. Patrick, and J. A. Dani. 1994. Improved technique for studying ion channels expressed in *Xenopus* oocytes, including fast superfusion. *Biophys. J.* 67:395–401.

Crane, R. K. 1977. The gradient hypothesis and other models of carrier-mediated active transport. *Rev. Physiol. Biochem. Pharmacol.* 78: 99–159.

Crane, R. K., D. Miller, and I. Bihler. 1961. The restrictions on possible mechanisms of intestinal active transport of sugars. *In:* Membrane Transport and Metabolism. A. Kleinzeller and A. Kotyk, editors. Academic Press, New York. 439–449.

Hediger, M. A., M. J. Coady, T. S. Ikeda, and E. M. Wright. 1987. Expression cloning and cDNA sequencing of the Na^+/glucose co-transporter. *Nature (London).* 330:379–381.

Hediger, M. A., E. Turk, and E. M. Wright. 1989. Homology of the human intestinal Na^+/glucose and *E. coli.* Na^+/proline cotransporters. *Proc. Natl. Acad. Sci. USA.* 86:5748–5752.

Hediger, M. A., and D. B. Rhoads. 1994. Molecular physiology of sodium-glucose cotransporters. *Physiol. Rev.* 74:993–1026.

Hilgemann, D. W. 1994. Channel-like function of the Na, K pump probed at microsecond resolution in giant membrane patches. *Science.* 263: 1429–1432.

Hilgemann, D. M., D. A. Nicoll, and K. D. Philipson. 1991. Charge movement during Na^+ translocation by native and cloned cardiac Na^+/Ca^{2+} exchanger. *Nature (London).* 352:715–718.

Hirayama, B. A., D. D. F. Loo, and E. M. Wright. 1994. Protons drive sugar transport through the Na^+/glucose cotransporter (SGLT1). *J. Biol. Chem.* 269:21,407–21,410.

Jalal, F., M. J. Coady, M. Cartier, B. Wallendorff, G. Lemay, and J.-Y. Lapointe. 1996. Functional studies of a chimeric Na^+/glucose cotransporter containing portions of SMIT and SGLT1. *FASEB J.* 10:A89.

Kimmich, G. A., and J. Randles. 1988. Na^+-coupled sugar transport: membrane potential-dependent K_m and K_i for Na^+. *Am. J. Physiol.* 255:C486–C494.

Klamo, E. M., and M. P. Kavanaugh. 1995. Kinetics of electrogenic cationic amino acid transporters. *Biophys. J.* 68:A438.

Lee, W. S., Y. Kanai, R. G. Wells, and M. A. Hediger. 1994. The high affinity Na^+/glucose cotransporter. *J. Biol. Chem.* 269:12,032–12,039.

Loo, D. D. F., F. Benzanilla, and E. M. Wright. 1994. Two voltage-dependent steps are involved in the partial reactions of the Na^+/glucose cotransporter. *FASEB J.* 8:A344.

Loo, D. D. F., A. Hazama, S. Supplisson, E. Turk, and E. M. Wright. 1993. Relaxation kinetics of the Na^+/glucose cotransporter. *Proc. Natl. Acad. Sci. USA.* 90:5767–5771.

Mackenzie, B., M. P. Heiermann, D. D. F. Loo, J. E. Lever, and E. M. Wright. 1994. SAAT1 is a low affinity Na^+/glucose cotransporter and not an amino acid transporter. *J. Biol. Chem.* 269:22,488–22,491.

Murer, H., and U. Hopfer. 1974. Demonstration of electrogenic Na^+-dependent D-glucose transport in intestinal brush border membranes. *Proc. Natl. Acad. Sci. USA.* 71:484–488.

Nakao, M., and D. C. Gadsby. 1986. Voltage dependence of Na translocation by the Na/K pump. *Nature (London).* 323:628–630.

Ohta, T., K. T. Isselbacher, and D. B. Rhoads. 1990. Regulation of glucose transporters in LLC-PK1 cells: effects of D-glucose and monosaccarides. *Mol. Cell. Biol.* 10:6491–6499.

Parent, L., S. Supplisson, D. D. F. Loo, and E. M. Wright. 1992a. Electrogenic properties of the cloned Na^+/glucose cotransporter: I. Voltage-clamp studies. *J. Membrane Biol.* 125:49–62.

Parent, L., S. Supplisson, D. D. F. Loo, and E. M. Wright. 1992b. Electrogenic properties of the cloned Na^+/glucose cotransporter: II. A transport model under nonrapid equilibrium conditions. *J. Membrane Biol.* 125:63–79.

Quick, M. W., J. Naeve, N. Davidson, and H. A. Lester. 1992. Incubation with horse serum increases viability and decreases background neurotransmitter uptake in *Xenopus* oocytes. *Biotechniques.* 13:357–361.

Rakowski, R. F. 1993. Charge movement by the Na/K pump in *Xenopus* oocytes. *J. Gen. Physiol.* 101:117–144.

Restrepo, D., and G. A. Kimmich. 1985. Kinetic analysis of mechanism of intestinal Na^+-dependent sugar transport. *Am. J. Physiol.* 248: C498–C509.

Schultz, S. G., and P. F. Curran. 1970. Coupled transport of sodium and organic solutes. *Physiol. Rev.* 50:637–718.

Semenza, G., M. Kessler, M. Hosang, J. Weber, and U. Schmidt. 1984. Biochemistry of the Na^+, D-glucose cotransporter of the small intestinal brush-border membrane. *Biochim. Biophys. Acta.* 779:343–379.

Taglialatela, M., L. Toro, and E. Stefani. 1992. Novel voltage clamp to record small, fast currents from ion channels expressed in *Xenopus* oocytes. *Biophys. J.* 61:78–82.

Tarpey, P. S., S. P. Shirazi-Beechey, and R. B. Beechey. 1994. Molecular characterization of the Na^+/glucose co-transporter from the sheep parotid gland acinar cell. *Biochem. Soc. Trans.* 22:264S.